

INFLUENCE OF ANATASE TITANIUM DIOXIDE NANOTUBE ARRAYS ON HUMIDITY SENSOR SYNTHESIZED BY ELECTROCHEMICAL ANODIZATION

Najwa Ezira Ahmed Azhar^{a,b}, Salifairus Mohammad Jafar^{b,c}, Nurul Hidah Sulimai^{b,c}, Mohamad Firdaus Malek^b, Mohamad Hafiz Mamat^a, Shafinaz Sobihana Shariffudin^a, Maryam Mohammad^{b,c,d}, Kevin Alvin Eswar^{b,c,e}, Ahmad Shuhaimi Abu Bakar^f, Salman A. H. Alrokayan^g, Haseeb A. Khan^g, M. Rusop^{a,b*}

Article history

Received
16 November 2021
Received in revised form
15 June 2022
Accepted
25 July 2022
Published Online
31 October 2022

*Corresponding author
rusop@uitm.edu.my

^aNANO-ElecTronic Centre, School of Electrical Engineering, College of Engineering, Universiti Teknologi MARA, 40450 Shah Alam, Selangor, Malaysia

^bCentre for Functional Materials and Nanotechnology, Institute of Science, Universiti Teknologi MARA, 40450 Shah Alam, Selangor, Malaysia

^cFaculty of Applied Sciences, Universiti Teknologi MARA, 40450 Shah Alam, Selangor, Malaysia

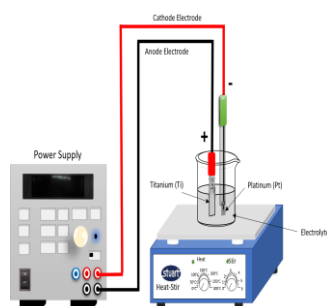
^dFaculty of Applied Sciences, Universiti Teknologi MARA (UiTM) Perak Branch, Tapah Campus, 35400 Tapah Road, Perak, Malaysia

^eFaculty of Applied Sciences, Universiti Teknologi MARA Sabah Branch Tawau Campus, 91032 Tawau, Sabah, Malaysia

^fLow Dimensional Materials Research Centre, Department of Physics, Faculty of Science, University of Malaya, 50603 Kuala Lumpur, Malaysia

^gResearch Chair for Biomedical Applications of Nanomaterials, Deanship of Scientific Research, King Saud University, 245 Riyadh 11454, Kingdom of Saudi Arabia

Graphical abstract



Abstract

Humidity sensors have become increasingly important and widely used to improve the quality of life and industrial processes. Over the past decades, titanium dioxide (TiO_2) has received wide attention in many promising areas such as sensors, solar cells, and photocatalytic. However, TiO_2 required high operating conditions such as high temperatures to examine the crystalline stability phase. This study focuses on highly ordered titanium dioxide nanotube arrays (TiO_2 NTAs) film synthesized using the electrochemical anodization method. Annealing temperature effect on the fabricated TiO_2 NTAs was investigated. An electrolyte solution was prepared by mixing ammonium fluoride (0.3 wt%) and ethylene glycol (25 ml) with deionized water (2 vol%). Titanium (Ti) sheet was anodized at 35 V for 120 minutes. The films were annealed from 350 °C to 550 °C. FESEM images showed the diameter size of TiO_2 NTAs film decreases as the annealing temperatures increases. Results had also shown that the average diameter annealed at 450 °C was around ~50.82 nm while the XRD pattern demonstrated TiO_2 NTAs exhibiting an anatase phase with a prominent (101) peak recorded for the sample prepared at 450 °C with a high crystallite size of 29.17 nm. The calculated optical band gap annealed at 450 °C (3.24

eV) is comparable with other literature. The current-voltage characteristic of TiO₂ NTAs film reported a high current for 450 °C (1.12 x 10⁻⁵ A) with a conductivity of 0.048 S.cm⁻¹ and high sensitivity (287.72).

Keywords: TiO₂ NTAs, electrochemical anodization, annealing temperature, physical properties, humidity sensor

Abstrak

Penderia kelembapan telah menjadi semakin penting dan digunakan secara meluas untuk meningkatkan kualiti hidup dan proses diindustri. Pada dekad yang lalu, titanium dioksida (TiO₂) telah mendapat perhatian yang meluas dalam banyak bidang seperti penderia, sel suria dan fotokatalitik. Walau bagaimanapun, TiO₂ memerlukan keadaan operasi pada suhu tinggi untuk fasa kestabilan kristal. Kajian ini memberi tumpuan kepada susunan filem titanium dioksida nanotube (TiO₂ NTA) yang disintesis menggunakan kaedah penganodan elektrokimia. Kesan suhu sepuhlindap TiO₂ NTA telah dikaji. Larutan elektrolit disediakan dengan mencampurkan ammonium fluorida (0.3 wt%) dan etilena glikol (25 ml) dengan air ternyahion (2 vol%). Kepingan Titanium (Ti) dianodkan pada 35 V selama 120 minit. Filem telah disepuhlandap pada 350 °C hingga 550 °C. Keputusan menunjukkan saiz diameter filem TiO₂ NTAs berkurangan apabila suhu sepuhlindap meningkat. Keputusan juga menunjukkan bahawa purata diameter yang disepuhlandap pada 450 °C adalah sekitar ~50.82 nm manakala spektrum XRD menunjukkan TiO₂ NTA mempamerkan fasa anatase dengan puncak yang ketara (101) direkodkan untuk sampel yang disediakan pada 450 °C dengan saiz kristal 29.17 nm. Jurang jalur optik yang dipanaskan pada 450 °C (3.24 eV) adalah setanding dengan kajian lepas. Pencirian arus voltan terhadap filem TiO₂ NTAs menunjukkan nilai yang tinggi untuk 450 °C (1.12 x 10⁻⁵ A) dengan kekonduksian 0.048 S.cm⁻¹ dan sensitiviti (287.72).

Kata kunci: TiO₂ NTA, penganodan elektrokimia, suhu sepuhlindap, sifat fizikal, sensor kelembapan

© 2022 Penerbit UTM Press. All rights reserved

1.0 INTRODUCTION

Titanium dioxide (TiO₂) is a semiconductor material that can form nanostructures and produce valuable optical and electrical properties. TiO₂ had been used in a range of industrial and consumer products. The TiO₂ can be tailored into various shapes such as nanoparticles, nanorods, nanowires, and nanotubes. [1–4]. Due of each tube's growth array to the surface, nanotubes have attracted the most attention among these nanostructures. The titanium dioxide nanotube arrays (TiO₂ NTAs) have a unique nanoarchitecture, large surface area, and high mechanical stability than TiO₂ nanoparticles [5].

TiO₂ NTAs can be synthesized using different types of methods such as electrochemical anodization and hydrothermal. Electrochemical anodization is an electrolytic technique capable of increasing the oxide layer thickness. Anodization is the facile practical approach due to its highly ordered and vertically oriented [6, 7]. All favorable properties render TiO₂ NTAs suitable for various applications such as photocatalytic, sensors, and dye-sensitized solar cells [8-10].

TiO₂ consists of three crystalline phases known as anatase (3.2 eV), rutile (3.0 eV), and brookite. TiO₂ transformation phases from amorphous to anatase and then to the rutile phase depends on the annealing temperature applied [11]. Based on three

polymorphs, the anatase and brookite are metastable, while rutile is the most stable polymorphs. The anatase and rutile phases are commonly used and applied in electronic device applications. However, TiO₂ required high operating conditions such as high temperatures to examine the crystalline stability phase. In research, the anatase is usually found in nanostructured TiO₂ and is active in oxide processes [12]. Mostly, Varghese and co-workers (2003) found the unstable crystallinity phase in low operating temperatures [13]. This researchers revealed the potential applications depend on the isomorph and crystallinity at desired operating conditions. The amorphous TiO₂ NTAs can crystallize to form anatase phase when immersed at low temperature treatment (>100°C) by a facile immersion method [14]. They reported that by using low temperature is a new route for crystalline TiO₂ NTAs. However, the optimization of TiO₂ NTAs using low temperature crystallization is still limited [15, 16].

Generally, the TiO₂ NTAs are required heat treatment at high temperature to sustain crystallization. Therefore, by fabrication of TiO₂ based humidity sensor properties it could certainly promotes multifunctional sensitivity behaviour and high efficiencies applications that may led to newer opportunities in disciplines as diverse as physics, chemistry, biology, medicine and engineering. Due to the metal oxide-based semiconductor produced

at lower cost method with higher productivity and performances, TiO₂ film can also be used in domestic, industrial, electronics and semiconductor and residential application in addition to the fabrication of humidity sensor device. Industries like chemical, refineries, metal, or others where furnaces are also in need humidity sensors as high humidity reduces the amount of oxygen present in the air.

In this study, the synthesis of TiO₂ NTAs films will be anodized using the electrochemical anodization method for the humidity sensor. The physical properties of TiO₂ NTAs films deposited at different annealing temperatures were investigated.

2.0 METHODOLOGY

Titanium (Ti) sheet (0.25 mm thick, 99.9 percent pure, Sigma-Aldrich) was chosen as the substrate and cleaned for 10 minutes in an ultrasonic water bath with acetone, methanol, and deionized (DI) water. In order to create an electrolyte solution, ammonium fluoride (0.3 wt%), ethylene glycol (25 ml), and DI water were mixed together and aged for 30 minutes. The anode and cathode electrodes were selected as platinum (Pt) and Ti sheets, respectively where they are submerged and anodized for 120 minutes in the electrolyte solution. The electrochemical anodization process was then used to anodize the Ti sheet at a 35V applied voltage. Finally, the anodized TiO₂ samples were annealed for 60 minutes at temperatures of 350° to 450°C.

The surface morphology and element analysis of TiO₂ NTAs film was analyzed by field emission scanning electron spectroscopy, FESEM (JEOL JSM-J600F), and (Zeiss Supra 40 VP). Determination of the crystalline structure TiO₂ NTAs film was obtained using X-Ray diffractometer, XRD (Rigaku (D/MAX-2000)). The optical properties of the TiO₂ NTAs film were investigated by ultraviolet-visible (UV-Vis) spectroscopy in the wavelength ranges between 200 – 1500 nm based on diffused reflectance spectroscopy (Varians 5000). The gold (Au) metal was chosen as metal electrode and deposited onto TiO₂ films (thickness: 60 nm) for current-voltage (I-V) measurement using sputter coater (EMITECH K550X). Electrical characteristics of TiO₂ NTAs films were measured using two-point probe (I-V) measurement. The humidity sensing performance of TiO₂ NTAs films was tested inside a humidity chamber (ESPEC-SH261) using Keithley 2400 sensor measurement system. This humidity system has been reported by other literature [17].

3.0 RESULTS AND DISCUSSION

Figures 1(a)–(d) show FESEM images of TiO₂ NTAs films (top view). The average diameters of the as-deposited, 350 °C, 450 °C, and 550 °C nanotube samples are 68.17 nm, 52.14 nm, 50.82 nm, and 48.23

nm, respectively, as shown in Table 1. It was discovered that the morphology of the as-deposited TiO₂ NTAs films generated as in Figure 1(a) is not well pronounced and non-homogeneous, with an abundance of nano-prickles formed on the top surface of the sample. This could be owing to inadequate atomic kinetic energy to overcome surface energy, resulting in built-in hydroxides on the surface of the nanotube's walls as well as a residual porous TiO₂ layer from the early phases of production [18, 19].

On the other hand, it can be seen in Figure 1(b) that after being annealed at 350 °C, the top surface of the sample has a more uniformed nanotube structure and the production of nano-prickles is not as apparent, indicating complete removal of residual F-ions and reduced hydroxide layer on the surface which tallies with previous studies done by other researchers [20] and this evidence can be proven in EDX image (Figure 3). Some other researcher studies the watching process using ultrasonic method affect the F- residue from electrolytes before annealing treatment [21]. Collectively, the diameter of nanotubes for annealed samples is in the range of 48 - 52 nm. This diameter is smaller than the As-deposited sample, with a larger average diameter of 68.17 nm. The changes of diameter because of the nucleation site increase and sufficient energy to produce more stable of nanotubes [22].

Figure 2 depicts a cross-sectional view of TiO₂ NTAs annealed at 450 °C, revealing that TiO₂ NTAs growth is perpendicular to the substrate surface. The measured thickness of TiO₂ NTAs film that annealed at 450 °C was 3.49 μm. As a result, the direct process of thermal oxidation caused the heat treatment to directly influence the oxide layer [23]. The performance of humidity sensor can be determined by its structural properties such large surface area and controlled morphology as mentioned by Steele et al., 2008 [24].

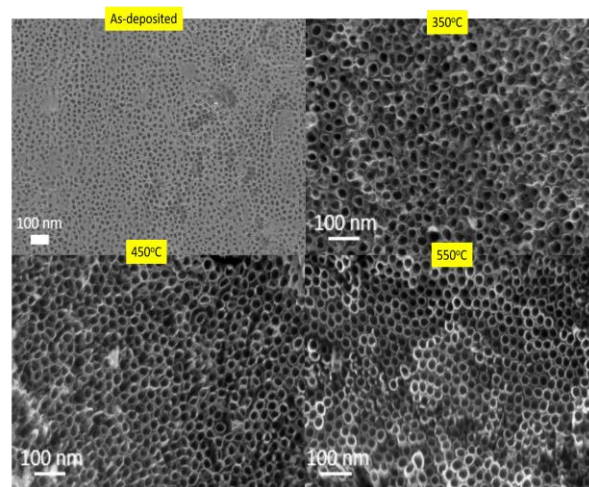


Figure 1 Surface morphologies of synthesized TiO₂ NTAs film by electrochemical anodization (a) as-deposited, and annealed at (b) 350°C, (c) 450°C and (d) 550°C

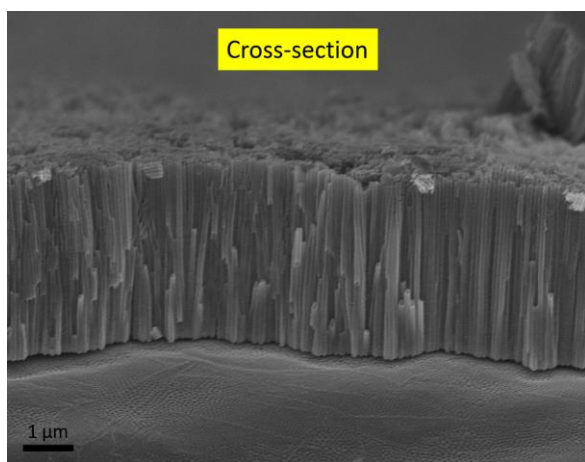


Figure 2 Cross-section of TiO₂ NTAs film annealed at (a) 450°C

Table 1 Average diameter size of TiO₂ NTAs films annealed at different temperatures

Annealing Temperature (°C)	Diameter Size (nm)	Standard Deviation
As-deposited (27)	68.17	2.92
350	52.14	7.72
450	50.82	3.51
550	48.23	3.28

Elemental analysis of TiO₂ NTAs film was annealed at 450 °C, as represented in Figure 3. The element analysis shows the oxygen (O) and Ti elements were detected via the electrochemical anodization method. The atomic percentages of Ti and O elements are 36.93% and 63.07%, respectively. There is no impurity detected through this film.

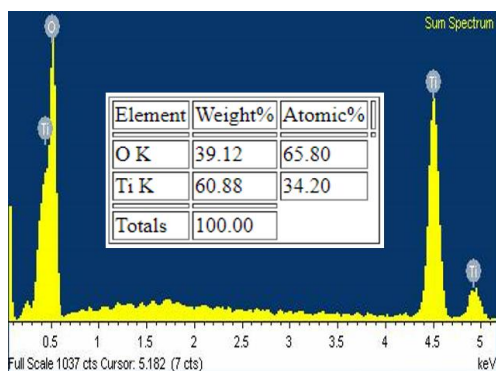


Figure 3 Element analysis of TiO₂ NTAs film annealed at 450°C

The crystalline structure of TiO₂ NTAs film was reflected by XRD spectra as shown in Figure 4 where obtained peaks are in the range of 20° to 85°. The patterns identified two forms of anatase and rutile phases. The peaks of (101), (004), (200), (105), (204), (220), (301), and (303) planes correspond to the anatase phase (JCPDS Card No. 00-004-0477) whereas the (110) plane refers to the rutile phase (JCPDS Card No. 00-004-0551). The detection peaks for (100), (002), and (101) planes specify the Ti pattern (JCPDS Card No. 00-044-1294).

The anatase peaks at $2\theta = 25.3^\circ$, 53.1° , and 70.8° were more prominent in the as deposited film and at 350°C, 450°C, and 550°C annealed films. Notably, rutile peak detection also was attained at annealing temperature of 550°C. However, at 350°C and 450°C annealing temperature, no rutile phase peaks can be found in the films. The rutile peak was existed when the TiO₂ films were annealed at higher temperature (> 500°C). To compute the crystallite size of TiO₂ NTAs films from the widening of the (101) plane diffraction peak at 25.3°, the Debye-Scherrer's formula was used as per below equation [25]:

$$D = k\lambda / (\beta \cos \theta) \quad (1)$$

where β is the full width at half maximum (FWHM) of the plane in radians, k is constant (0.9), λ is the wavelength of the 1.54 Å, and θ is the Bragg's angle in degrees. Based on the Figure 4, the FWHM can be determined by the distance between the curve points at the peak half maximum level. On a data graph, vertical line from the peak maximum to baseline was drew. The length was measured along the line and divide by 2 to find the center of the line.

The crystallite size of the as-deposited and annealed samples was listed in Table 2. The crystallite size for the rutile phase at the temperature of 550°C was calculated to be 12.86 nm. Additionally, it is evident that the crystallite size for the anatase phase is greater as the temperature increases and starts to decline at 550°C annealing temperature. The crystallite size (29.175 nm) also increases as the temperature increased up to 450°C. These can be attributed to thermally promoted crystallite growth [26]. Therefore, the improvement in crystalline quality is caused by the increase in crystallite size by atomic arrangement during phase transformations toward an energetically more favorable equilibrium state. Nevertheless, as reported by Varghese *et al.* (2003), the crystallite size was reduced because of atom rearrangement, and the phase transition from anatase to rutile had taken place at high annealing temperatures [13]. As a result, the sample that was annealed at 450°C had a substantial impact on the crystal structure and displayed good crystallinity.

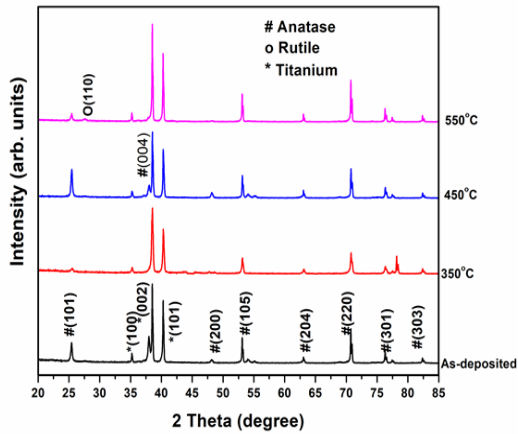


Figure 4 Crystalline structure of TiO₂ NTAs film annealed at As-deposited, 350°C, 450°C and 550°C

Table 2 Crystallite size of TiO₂ NTAs films annealed at different temperatures

Annealing Temperature (°C)	FWHM (101) peak	Crystallite Size, D (nm)	
		Anatase 25.3°	Rutile 27.5°
As-deposited	0.41949	19.4	-
350	0.39575	20.6	-
450	0.27915	29.2	-
550	0.31063	26.2	12.8

Investigation of band gap energy on TiO₂ NTAs films was studied through UV-Vis spectroscopy by obtaining diffuse reflectance spectroscopy (DRS), as shown in Figure 5. The average reflectance of 350°C, 450°C, and 550°C is 16.5%, 22.5%, and 15.3%, respectively. The TiO₂ layer absorbs the incident light at the UV region (350 nm). At lower wavelength shows the reflectance edge decreased due to electronic transition between valance and conduction bands [27, 28]. The reflectance edge of the annealed sample showed redshift caused by the structural phase change related to the modification of the phase transformation and crystalline size [29]. The light scattering of TiO₂ at the visible region showed broad peaks due to the impact of the annealing treatment of nanotubes [30]. The specular reflectance of the samples in the 700–800 nm range has a significant upward trend for different angles and polarizations. This phenomenon probably comes from the effect of the nano-topography of titanium dioxide. The band gap of TiO₂ NTAs films was calculated using Kubelka-Munk formula is given by Equation 2 [29].

$$F(R(h\nu)) = (1 - R(h\nu))/2R(h\nu) \tag{2}$$

where F(R(hν)) is the Kubelka-Munk function, and R is the reflectance of TiO₂ NTAs. Tauc's plot determined

the band gap by employing the linear correlation between Kubelka-Munk function.

$$[F(R)h\nu]^{1/2} = A(h\nu - E_g) \tag{3}$$

The band gap energy value of As-deposited, 350°C, 450°C, and 550°C films were calculated at about 4.34 eV, 3.25 eV, 3.24 eV, and 3.25 eV, respectively. The As-prepared sample showed the highest band gap energy value and starts to decrease as the annealing temperature increases. This might be due to the increment of the crystallite size and film density manipulation [31]. Film density can be related to the process energy of formation thin film. The energy increase makes the film density increased and influence the resulting structural and optical properties [32, 33]. The film density condition depending on the annealing temperature. Hanini *et al.* (2013) revealed that the decrease in band gap of TiO₂ with annealing temperature can be the densification of the films [34]. Due to the nanotubes highly ordered, densely packed structure, the annealed samples likewise displayed comparable band gap energy levels [29, 35]. In other words, the morphology of nanotubes may be related to the variance in band gap energy. The crystallinity, crystal structure, grain, and particle size of the film are other parameters that affect the band gap [36].

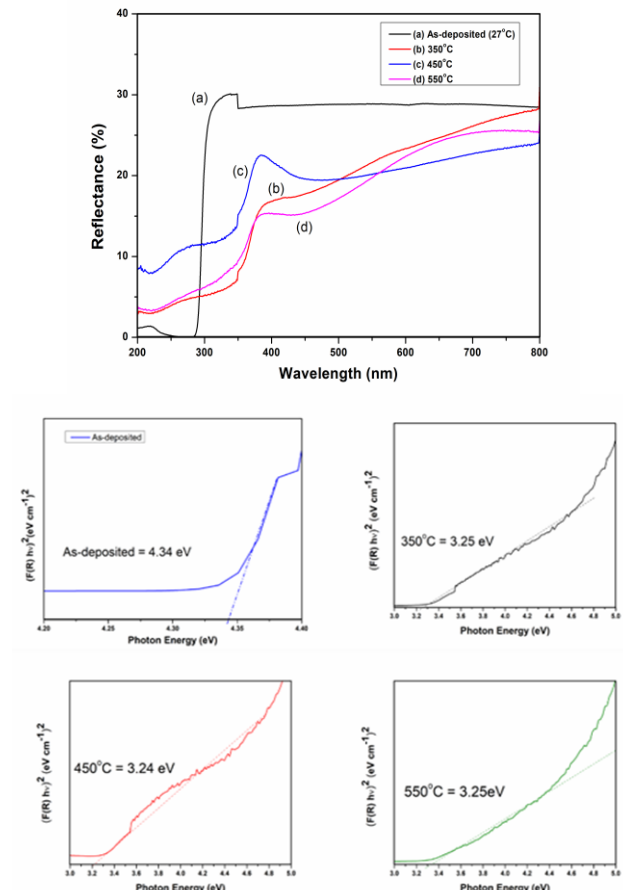


Figure 5 Reflectance and band gap energy of TiO₂ NTAs film annealed at As-deposited, 350°C, 450°C and 550°C

Figure 6 displays the current-voltage (I-V) characteristic of the sample that was annealed between 350 and 550°C. At room temperature, the I-V measurement ranged from -0V to 6V. The forward current rises with voltage to 6V (11.2µA) and it can also be observed that the I-V curve exhibited linear and symmetric ohmic contact behaviour.

The voltage has an impact on the resistance between each pair of metal contacts. One crucial factor in determining the work function between the metal contact and TiO₂ films is the suitability of the metal contact material. Most common metal contact materials employed are gold (Au), platinum (Pt), and palladium (Pd). According to Musa *et al.* (2010), a relatively low work function of gold (Au) enables more electrons from TiO₂ sheets to move across the contact surface [37]. The resistivity of the films were determined using equation (4):

$$\rho = (V/I)(wt/L) \quad (4)$$

where ρ is the resistivity, V is supplied voltage, I is measured current, w is the electrode width, t is the thickness of film, and L is the length between the electrodes. The conductivity (σ) of the film can be determined using equation (5):

$$\sigma = 1/\rho \quad (5)$$

Resistivity and conductivity values of the TiO₂ NTAs films are tabulated in Table 3. The metal contact has affected the resistivity and conductivity of the TiO₂ film. Conductivity values shows gradually increased up to 450°C. However, when the temperatures were increased up to 550°C, the conductivity was significantly reduced. The improvement of conductivity values might be due to the charge carriers mobility as reported by Rajeswari *et al.*, (2020) [38]. Refer to Table 4, it found that the conductivity values of TiO₂ NTAs film is better than Rajeswari *et al.*, 2020, [38]. Therefore, the sample annealed at 450°C shows the highest conductivity value with 0.096 S.cm⁻¹. The good crystallinity and the band gap energy obtained at 450°C provides a large surface for electron for electron transmission between grains as stated by Senain *et al.*, 2010 [39]. From these results, the TiO₂ NTAs film at different annealing temperatures changes the electrical performance.

Refer to the I-V measurement, it can be seen that the current of the films increases with the increment of % RH. Figure 7(a) shows the humidity sensing of TiO₂ NTAs films annealed at different temperatures. Humidity chamber was used with different type level of humidity from 40 to 90% RH at room temperature where The RH was sustained at 40%. When the time reaches up to 100 seconds, the RH was changed to 90% to examine the absorption of humidity. Results shows current signal increasing steadily until it reaches 90% RH. Once the RH and current starts to decrease slowly from 90 to 40% RH, the desorption properties was determined.

The performance of TiO₂ NTAs films was explained based on sensitivity equation [40]:

$$S = R_{40}/R_{90} \quad (6)$$

where S is sensitivity, R₄₀ is resistance at 40% RH, and R₉₀ represents the resistance at 90% RH. The resistance values were calculated by using Ohm's Law.

Figure 7(b) displays the sensitivity value of annealed TiO₂ NTAs at various temperatures. It was found that the annealing temperatures had enhanced the sensitivity value, with 450°C sample having the greatest sensitivity of 287.72. The sensitivity value of our humidity sensor is also compared to other reported humidity sensors where it was discovered to be superior to those of Aneesh and Khijwania (2012) and Ghadir *et al.*, 2016 [41, 42]. This might also be attributed to the morphological, structural, optical and electrical properties of the TiO₂ NTAs. The surface either open or pore size had contributed in humidity sensitivity. The annealed sample at 450°C was measured by exposing to various % RH as tabulated in Table 4. These result shows the sample is sensitive to the different RH with the pattern of increment observed from these values. As more water molecules in the sample ionise, more H⁺ ions become accessible for protonic conduction, which improve in sensitivity. The sample's sensitivity rises because more charge carrier in the form of electron or ions are available in the thin films [40]. However, the sensitivity substantially deteriorated when the temperature increases up to 550°C. This is because of pore size and distribution on the surface of sensing samples can also influence the production of chemical adsorption and physical adsorption layers [43]. Due to the physical contact between the surface and the water, it can also be confirmed that the TiO₂ NTAs annealed at 450°C have good sensitivity [44]. These enhanced properties cause fast adsorption and desorption of water molecules, which results in rapid response and recovery times as reported by Jyothilal *et al.*, (2020) and Sun *et al.*, 2018 [40, 45].

Figure 8 shows repeatability behaviour of TiO₂ NTAs film-based humidity sensor at 450°C. The repeatability was measured at 4 response cycles. The response cycles were very stable and indicates good repeatability behavior [45].

At low relative humidity, oxygen from the environment might attract to the sensor surface, resulting in electron entrapment [40]. Adsorbed oxygen ion was generated by the interaction of oxygen molecules. The concentration of free carriers in this film has been reduced. The trapped electron was released back to the surface of the TiO₂ NTAs film due to chemical adsorption of water molecules. Before the RH level was raised over 40 %, the electron trapping and water molecule adsorption reactions occurred at the same rate. The current signal is consistent. The adsorption process gradually increased as the RH level increased, forming physical

adsorption water layers. Due to the high electrostatic force in the chemisorbed layer, the physical adsorption water layer dissociates into H_3O^+ and OH^- ions.

The H^+ from H_3O^+ continually jumps from one water molecule to another and becoming the dominant charge carriers which are the source of electrical conduction [42]. This mechanism called as Grotthuss chain as shown in Figure 9. Based on the I-V measurement, the sample annealed at 450 °C that produced highest free carriers which give rise to high water molecule adsorption and leading to large current change ratio. Water molecules begin to condense between the pore channels of the TiO_2 NTAs at high RH levels. The capillary condensation of water molecules facilitated the free discharge of conducting ions across each of the nanotubes [42].

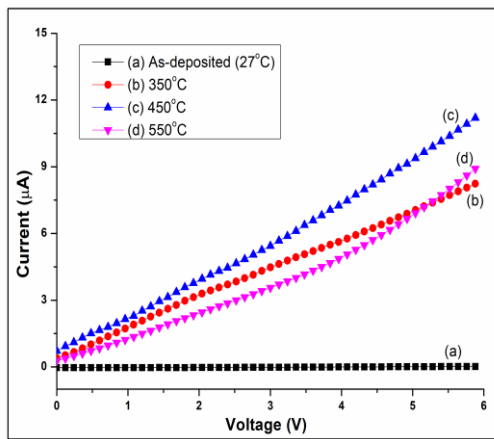


Figure 6 Current-voltage (I-V) measurement of TiO_2 NTAs film annealed at 450 °C

Table 3 Resistivity and conductivity of TiO_2 NTAs films annealed at different temperatures

Annealing Temperature (°C)	Resistivity ($\Omega \cdot cm$)	Conductivity ($S \cdot cm^{-1}$)
As-deposited (27)	68.11×10^1	0.001
350	12.70	0.078
450	10.37	0.096
550	23.03	0.043

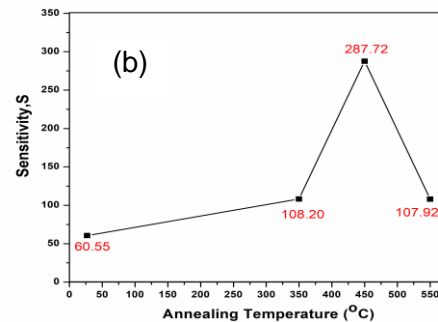
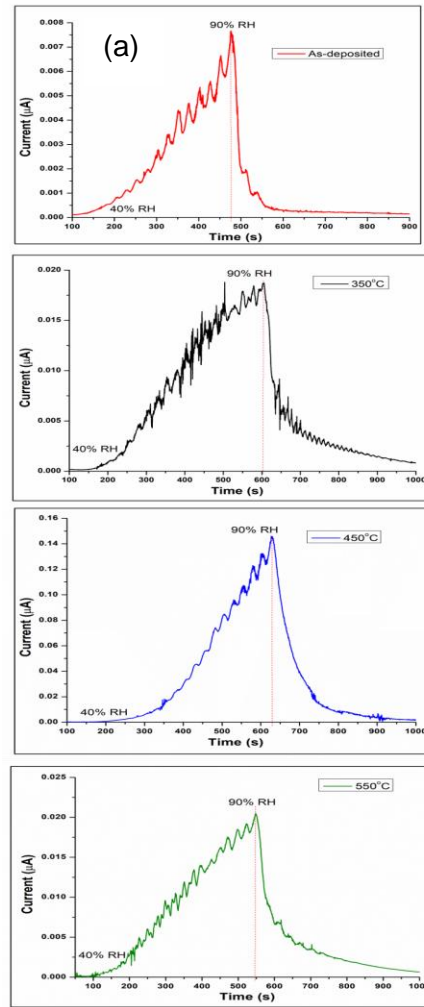


Figure 7 Humidity detection of TiO_2 NTAs film annealed at 350 to 450 °C with bias voltage of 5 V and (b) the sensitivity of TiO_2 NTAs at different annealing temperatures

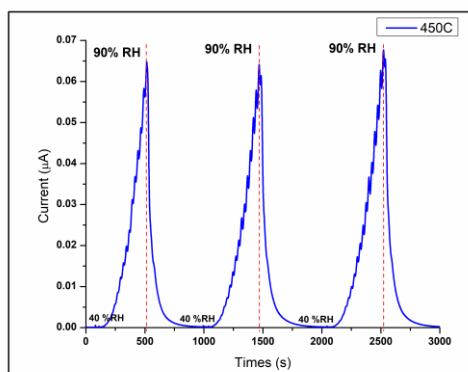


Figure 8 Repeatability behavior of TiO₂ NTAs film annealed at 450 °C

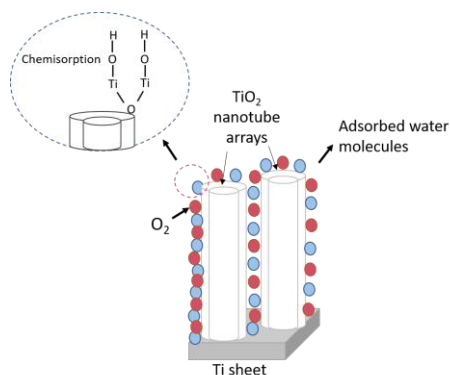


Figure 9 Humidity sensor mechanism

Table 4 Sensitivity of TiO₂ NTAs films annealed at 450 °C at various % RH

RH (%)	Sensitivity
50	2.00
60	2.68
70	8.69
80	42.04
90	287.72

4.0 CONCLUSION

Titanium dioxide nanotube arrays films were successfully prepared at different annealing temperatures via the electrochemical anodization method. The surface morphology demonstrated that when the annealing temperature increases, the diameter of produced TiO₂ NTAs decreased and ranged between 41 and 76 nm as well as improvement on the nanotubes more well-organized structure. This was also supported by XRD results where the TiO₂ NTAs displayed the anatase phase between 350 °C and 450 °C, and the transformation from anatase to rutile phase was discovered at 550 °C. The anatase phase's largest crystallite size (29.175

nm) was produced by annealing at 450 °C. When the sample was annealed from 350 to 550 °C, the optical characteristics revealed that the band gap energy values of TiO₂ NTAs were in the range of 3.24 to 3.25 eV. Additionally, gold (Au) metal contact was used and the generated film's conductivity was determined to be 0.048 S.cm⁻¹. The 450 °C-annealed TiO₂ NTAs also have excellent sensitivity value of 287.72. These findings indicated a potential material for humidity sensor detection and revealed that the properties of synthetic TiO₂ NTAs films are considerably influenced by annealing temperature.

Acknowledgement

This work is financially supported by GIP grant (600-RMC/GIP 5/3 (035/2021) and FRGS grant (600-IRMI/FRGS-RACER 5/3 (102/2019)), Institute of Research Management & Innovation (IRMI), Universiti Teknologi MARA (UiTM), Ministry of Education Malaysia. The authors also like to thank Mrs. Ts. Irmaizatussyehdany Bunyamin (UiTM Senior Research Officer), Mr Muhamad Faizal Abd Halim (UiTM Assistant Research Officer), and Mr. Mohd Azlan Jaafar (UiTM Assistant Engineer) for their kind support for this research.

References

- [1] Asim, M., Ahmad, K., Khaliq, N., Khan, Y., Aftab, M., Waheed, A., Shah, A., Mahmood, A., and Ali, G. 2018. Effect of Electrochemical Reduction on The Structural and Electrical Properties of Anodic TiO₂ Nanotubes. *Current Applied Physics*. 18: 297-303. DOI: <https://doi.org/10.1016/j.cap.2018.01.001>.
- [2] Othman, M. A., Amat, N. F., Ahmad, B. H., and Rajan, J. Electrical Conductivity Characteristic of TiO₂ Nanowires from Hydrothermal Method. *Journal of Physics Conference Series*. 495: 012027. DOI: <https://doi.org/10.1088/1742-6596/495/1/012027>.
- [3] Saravanan, P., Ganapathy, M., Charles, A., Ramilselyan, S., and Jayesekaran, R. 2016. Electrical Properties of Green Synthesized TiO₂ Nanoparticles. *Advances in Applied Science Research*. 7(3): 158-168.
- [4] Yusoff, M., Mamat, M. H., Ismail, A. S., Malek, M. F., Zoolfakar, A. S., Suriani, A. B., Ahmad, M. K., Nayan, N., Shameem Banu, I. B., and Rusop, M. 2018. Low-Temperature-Dependent Growth of Titanium Dioxide Nanorod Arrays in An Improved Aqueous Chemical Growth Method for Photoelectrochemical Ultraviolet Sensing. *Journal of Materials Science: Materials in Electronic*. 1-16. DOI: <https://doi.org/10.1007/s10854-018-0371-8>.
- [5] Jun, W., and Zhiquan, L. 2009. Anodic Formation of Ordered TiO₂ Nanotube Arrays: Effects of Electrolyte Temperature and Anodization Potential. *Journal of Physical Chemistry C*. 113: 4026-4030. DOI: <https://doi.org/10.1021/jp811201x10.1016/j.apsusc.2014.01.086>.
- [6] Li, Y., Ma, Q., Han, J., Ji, L., Wang, J., Chen, and Wang, Y. 2014. Controllable Preparation, Growth Mechanism and The Properties Research of TiO₂ Nanotube Arrays. *Applied Surface Science*. 103-108. DOI: <https://doi.org/10.1016/j.apsusc.2014.01.086>.
- [7] Escada, A. L., Nakazato, R. Z., and Claro, A. P. R. A. 2017. Influence of Anodization Parameters in the TiO₂

- Nanotubes Formation on Ti-7.5Mo Alloy Surface for Biomedical Application. *Materials Research*. 20(5): 1282-1290.
DOI: <http://dx.doi.org/10.1590/1980-5373-MR-2016-0520>.
- [8] Galstyan, V., Comini, E., Faglia, G., and Sberveglieri. 2013. TiO₂ Nanotubes: Recent Advances in Synthesis and Gas Sensing Properties. *Sensors* 2013. 13: 14813-14838.
DOI: <https://10.3390/s131114813>.
- [9] Slamet, S., and Purwanto, W. W. 2015. Synthesis of TiO₂ Nanotubes by Using Combination of Sonication and Hydrothermal Treatment and Their Photocatalytic Activity for Hydrogen. *Reaktor*. 15(3): 205-212.
DOI: <https://10.14710/reaktor.15.3.204-211>.
- [10] Sreekantan, S., Arifah, K., Ly, N. T., Nguyen, V. C., Hoa, T., Rozana, M., Soaid, N. I., Wai, T., and Le, H. 2011. Formation of TiO₂ Nanotubes via Anodization and Potential Applications for Photocatalysts, Biomedical Materials, and Photoelectrochemical Cell. *Materials Science and Engineering*. 21: 012002.
DOI: <https://10.1088/1757-899X/21/1/012002>.
- [11] Iraj, M., and Kolahdouz, M. 2016. TiO₂ Nanotube Formation by Ti Film Anodization and Their Transport Properties for Dye-Sensitized Solar Cells. *Journal Material Science: Material Electron*. 27: 6496-6501.
DOI: <https://10.1007/s10854-016-4591-5>.
- [12] Zhang, B., Cao, S., Du, M., Ye, X., Wang, Y., and Ye, J. 2019. Titanium dioxide (TiO₂) Mesocrystals: Synthesis, Growth Mechanisms and Photocatalytic Properties. *Materials Science, Chemistry*. 9(9): 4-27.
DOI: <https://10.3390/catal9010091>.
- [13] Varghese, O. K., Gong, D., Paulose, M., Grimes, C. A. and Dickey, E. C. 2003. Crystallization and High-Temperature Structural Stability of Titanium Oxide Nanotube Arrays. *Journal of Materials Research*. 18(1):156-165.
DOI: <https://10.1557/JMR.2003.0022>.
- [14] Liao, Y., Que, W., Zhong, P., Zhang, J. and He, Y. A. Facile Method to Crystallize Amorphous Anodized TiO₂ Nanotubes at Low Temperature. *ACS Appl. Mater. Interfaces* 2011. 3: 2800-4.
DOI: 10.1021/am200685s.
- [15] Krengvirat, W., Sreekantan, S., Mohd Noor, A. F., Negishi, N., Tawamura, G., Muto, H., & Matsuda, A. 2013. Low-Temperature Crystallization of TiO₂ Nanotube Arrays via Hot Water Treatment and Their Photocatalytic Properties Under Visible-light Irradiation. *Materials Chemistry and Physics*. 137(3): 991-998.
DOI: <https://doi.org/10.1016/j.matchemphys.2012.11.013>.
- [16] Assaker, K., Carteret, C., Lebeau, B., Marichal, C., Vidal, L., Stebe, M.-J., and Blin, J.-L. 2014. Water-Catalyzed Low-Temperature Transformation from Amorphous to Semi-Crystalline Phase of Ordered Mesoporous Titania Framework. *ACS Sustainable Chem. Eng.* 2: 120-125
DOI: 10.1021/sc400323w.
- [17] Ismail, A. S., Mamat, M. H., Shameem Banu, I. B., Malek, M. F., Yusoff, M. M., Mohamed, R., Ahmad, W. R. W., Abdullah, M. A. R., Md. Sin, N. D., Suriani, A. B., Ahmad, M. K., and Rusop, M. 2018. Modulation of Sn Concentration in ZnO Nanorod Array: Intensification on the Conductivity and Humidity Sensing Properties. *Journal of Materials Science: Materials in Electronics*. 29(14): 12076-12088.
DOI: <https://doi.org/10.1007/s10854-018-9314-7>.
- [18] Abdulraheem, Y. M., Ghoraiishi, S., Arockia-Thai, L., Zachariah, S. K., and Ghannam, M. 2013. The Effect of Annealing on The Structural and Optical Properties of Titanium Dioxide Films Deposited by Electron Beam Assisted PVD. *Advances in Materials Science and Engineering*. 2013: 574738.
DOI: <https://10.1155/2013/574738>.
- [19] Wang, D., Liu, L., Zhang, F., Tao, K., Pippel, E., and Domen, K. 2011. Spontaneous Phase and Morphology Transformations of Anodized Titania Nanotubes Induced by Water at Room Temperature. *Nano Letters*. 11: 3649-3655. DOI: <https://10.1021/nl2015262>.
- [20] Sobieszczyk, S. 2009. Self-Organized Nanotubular Oxide Layers on Ti and Ti Alloys. *Advances in Materials Science*. 9(20): 26-41.
DOI: <https://10.2478/v10077-009-0008-y>.
- [21] Cao, C., Yan, J., Zhang, Y., and Zhao, L. 2016. Stability of Titania Nanotube Arrays in Aqueous Environment and the Related Factors. *Scientific Reports*. 6: 1-8.
DOI: <https://doi.org/10.1038/srep23065>.
- [22] Mehranpour, H., Askari, M., and Ghamsari, M. S. Nucleation and Growth of TiO₂ Nanoparticles. *Nanomaterials*. 2010. Tehran, Iran. Intech. Chapter 1.
DOI: 10.5772/25912.
- [23] Albu, S. P., Tsuchiya, H., Fujimoto, S., and Schmuki, P. 2010. TiO₂ Nanotubes – Annealing Effects on Detailed Morphology and Structure. *European Journal of Inorganic Chemistry*. 4351-4356.
DOI: <https://10.1002/ejic.201000608>.
- [24] Steele, J. J., Taschuk, M. T., and Brett, M. J. 2008. Nanostructured Metal Oxide Thin Films for Humidity Sensors. *IEEE Sensors Journal*. 8(8): 1422-1429.
DOI: <https://doi.org/10.1109/JSEN.2008.920715>.
- [25] Choudhury, B., Dey, M., and Choudhury, A. 2013. Defect Generation, d-d Transition and Band Gap Reduction in Cu-Doped TiO₂ Nanoparticles. *International Nano Letters*. 3: 25.
DOI: <https://10.1186/2228-5326-3-25>.
- [26] Haq, S., Rehman, W., Waseem, M., Javed, R., and Muhammad, R. 2018. Effect of Heating on the Structural and Optical Properties of - TiO₂ Nanoparticles: Antibacterial Activity. *Applied Nanoscience*. 8: 11-18.
DOI: <https://doi.org/10.1007/s13204-018-0647-6>.
- [27] Hendi, A. A., Alorainy, R. H., and Yakubhanoglu, F. 2014. Humidity Sensing Characteristics of Sn Doped Zinc Oxide Based Quartz Crystal Microbalance Sensors. *J. Sol. Gel Sci. Technol*. 72: 559-564.
DOI: <https://doi.10.1007/s10971-014-3473-7>.
- [28] Farzaneh, A., Mohammadzadeh, A., Esrafil, M. D., and Mermer, O. 2019. Experimental and Theoretical Study of TiO₂ Based Nanostructured Semiconducting Humidity Sensor. *Ceramics International*. 45(7): 8362-8369.
DOI: <https://doi.org/10.1016/j.ceramint.2019.01.144>.
- [29] Ali, S. M., and Khan, M. A. M. 2020. Annealing Effects on Structural, Optical and Electrical Properties of TiO₂/FTO Heterojunction. *Applied Physics A: Materials Science and Processing*. 126:468.
DOI: <https://doi.org/10.1007/s00339-020-03656-6>.
- [30] Lu, H., Huang, M., Shen, K. S., Zhang, J., Dong, C., Xiong, Z. G., Zhu, T., Wu, D. P., Zhang, B., and Zhang, X. Z. 2018. Enhanced Diffuse Reflectance and Microstructure Properties of Hybrid Titanium Dioxide Nanocomposite Coating. *Nanoscale Research Letters*. 13: 328.
DOI: <https://doi.org/10.1186/s11671-018-2763-3>.
- [31] Manickam, K., Muthusamy, V., Manickam, S., Senthil, T. S., Periyasamy, G. and Shanmugam, S. 2020. Effect of Annealing Temperature on Structural, Morphological and Optical Properties of Nanocrystalline TiO₂ Thin Films Synthesized by Sol-Gel Dip Coating Method. *Material Today: Proceedings*. 23: 68-72.
DOI: <https://10.1016/j.matpr.2019.06.651>.
- [32] Domaradzki, J., Kaczmarek, D., Prociow, E. L., and Radzinski, Z. J. 2011. Study of Structure Densification in TiO₂ Coatings Prepared by Magnetron Sputtering Under Low Pressure of Oxygen Plasma Discharge. *Acta Physica Polonica A*. 120(1): 49-52.
DOI: <https://doi.org/10.12693/APhysPolA.120.49>.
- [33] Xu, Y. N., Liu, M. N., Wang, M. C., Oloyede, A., Bell, J. M., and Yan, C. 2015. Nanoindentation Study of the Mechanical Behavior of TiO₂ Nanotube Arrays. *Journal of Applied Physics*. 118(14).
DOI: <https://doi.org/10.1063/1.4932213>.
- [34] Hanini, F., Bouabellou, A., Bouachiba, Y., Kermiche, F., Taabouche, A., Hemissi, M., and Lakhdari, D. 2013. Structural, Optical and Electrical Properties of TiO₂ Thin

- Films Synthesized by Sol–Gel Technique. *IOSR Journal of Engineering*. 3(11): 21-28.
DOI: 10.9790/3021-031112128.
- [35] Pishkar, N., Ghoranneviss, M., Ghoranneviss, Z., and Akbari, H. 2018. Study of the Highly Ordered TiO₂ Nanotubes Physical Properties Prepared with Two-Step Anodization. *Results in Physics*. 9: 1246-1249.
DOI: <https://10.1016/j.rinp.2018.02.009>.
- [36] Hsu, C. H., Chen, K. Te, Huang, P. H., Wu, W. Y., Zhang, X. Y., Wang, C., Liang, L. S., Gao, P., Qiu, Y., Lien, S. Y., Su, Z. B., Chen, Z. R., and Zhu, W. Z. 2020. Effect of Annealing Temperature on Spatial Atomic Layer Deposited Titanium Oxide and Its Application in Perovskite Solar Cells. *Nanomaterials*. 10(7): 1-15.
DOI: <https://doi.org/10.3390/nano10071322>.
- [37] Musa, M. Z., Sarah, M. S. P., Shariffudin, S. S., Mamat, M. H., and Rusop, M. 2010. A Study on Ohmic Contact of Different Metal Contact Materials on Nanostructured Titanium Dioxide (TiO₂) Thin Film. *International Conference on Electronic Devices, Systems and Applications (ICEDSA2010)*. 412-414.
DOI: <https://10.1109/ICEDSA.2010.5503028>.
- [38] Rajeswari, R., Venugopal, D., Jayabal, P., and Raj, A. D. 2020. Fabrication and Characterization of TiO₂ Thin Films and n-TiO₂/p-Si Junction Diodes via Dip Coating Technique. *Acta Physica Polonica A*. 138(3): 539-545.
DOI: <https://doi.org/10.12693/APhysPolA.138.539>.
- [39] Senain, I., Nayan, N., and Saim, H. 2010. Structural and Electrical Properties of TiO₂ Thin Film Derived from Sol-Gel Method Using Titanium (IV) Butoxide. *International Journal of Integrated Engineering (Issue on Electrical and Electronic Engineering)*. 29-35.
- [40] Jyothilal, H., Shukla, G., Walia, S., Kundu, S., and Angappane, S. 2020. Humidity Sensing and Breath Analyzing Applications of TiO₂ Slanted Nanorod Arrays. *Sensors and Actuators A: Physical*. 30:111758.
DOI: <https://10.1016/j.sna.2019.111758>.
- [41] Aneesh, R., and Khijwania, S. K. 2012. Titanium Dioxide Nanoparticle Based Optical Fiber Humidity Sensor with Linear Response and Enhanced Sensitivity. *Applied Optics*. 51(12): 2164-2171.
DOI: <https://10.1364/AO.51.002164>.
- [42] Ghadir, M., Gholami, M., Ahmad, H., and Chong, W. Y. 2016. Ultra-Sensitive Humidity Sensor Based on Optical Properties of Graphene Oxide and Nano-Anatase TiO₂. *PLoS One*. 11(4): 1-14.
DOI: <https://10.1371/journal.pone.0153949>.
- [43] Gapale, Dipak L., Bardapkar, Pranav P., Arote, Sandeep A., Dalvi, S., Baviskar, P., and Borse, Y. 2021. Humidity Sensing Properties of Spray Deposited Fe Doped TiO₂ Thin Film. *Journal of Semiconductors*. 42: 122805.
DOI: <https://10.1088/1674-4926/42/12/122805>.
- [44] Farzaneh, A., Esrafil, M. D., and Mermer, O. 2020. Development of TiO₂ Nanofibers Based Semiconducting Humidity Sensor: Adsorption Kinetics and DFT Computations. *Materials Chemistry and Physics*. 239: 121981.
DOI: <https://10.1016/j.matchemphys.2019.121981>.
- [45] Sun, L., Haidry, A. A., Fatima, Q., Li, Z., and Yao, Z. 2018. Improving the Humidity Sensing Below 30% RH of TiO₂ with GO Modification. *Materials Research Bulletin*. 99: 124-131.
DOI: <https://doi.org/10.1016/j.materresbull.2017.11.001>.